

Atroposelective iridium-catalyzed hydrogenation of *N*-arylindole ketones and heterobiaryl ketones via dynamic kinetic resolution enabled by planar-chiral tridentate PNO ligands

Tong Niu^{1,2}, Li-Xia Liu¹, Yu-Qing Bai¹, Hong-Wang Li¹, Bo Wu^{1*} & Yong-Gui Zhou^{1*}

¹State Key Laboratory of Catalysis, Dalian Institute of Chemical Physics, Chinese Academy of Sciences, Dalian 116023, China

²University of Chinese Academy of Sciences, Beijing 100049, China

Received January 17, 2025; accepted April 25, 2025; published online July 24, 2025

Asymmetric direct hydrogenation (ADH) is a straightforward and atom-economic methodology to achieve optically active compounds. The synthesis of chiral compounds bearing stereogenic centers has been well established. In contrast, the construction of atropisomers, especially atropisomers bearing multiple chiral elements, has sporadically been explored. Herein, we report an innovative atroposelective iridium-catalyzed hydrogenation of *N*-arylindole ketones and heterobiaryl ketones via dynamic kinetic resolution (DKR) based on a Lewis acid-base interaction between the nitrogen atom and the carbonyl group of ketones, providing C–N and C–C atropisomers bearing multiple chiral elements with excellent enantioselectivities, diastereoselectivities and yields. The lynchpin of the DKR-ADH process stands in the newly developed planar-chiral tridentate PNO ligand, which ensures the excellent control of enantioselectivity and diastereoselectivity simultaneously. The synthetic utilization of this protocol is proved through stereospecific transformation to a tridentate PNN ligand bearing axial and central chirality, which shows promising potential in iridium-catalyzed asymmetric hydrogenation of simple ketones.

asymmetric hydrogenation, dynamic kinetic resolution, atroposelective synthesis, atropisomers, planar-chiral tridentate PNO ligand

Citation: Niu T, Liu LX, Bai YQ, Li HW, Wu B, Zhou YG. Atroposelective iridium-catalyzed hydrogenation of *N*-arylindole ketones and heterobiaryl ketones via dynamic kinetic resolution enabled by planar-chiral tridentate PNO ligands. *Sci China Chem*, 2025, 68, <https://doi.org/10.1007/s11426-025-2729-y>

1 Introduction

Asymmetric hydrogenation has emerged as one of the most powerful tools for the construction of optically active pharmaceuticals, agrochemicals, flavors and fine chemicals in synthetic chemistry [1–9], as well as in industrial processes [10–12]. Taking advantage of its high efficiency and atom economy, systematic and significant achievements have been made, and tremendous chiral molecules have been synthesized through asymmetric transfer hydrogenation (ATH) and asymmetric direct hydrogenation (ADH). Among them, the

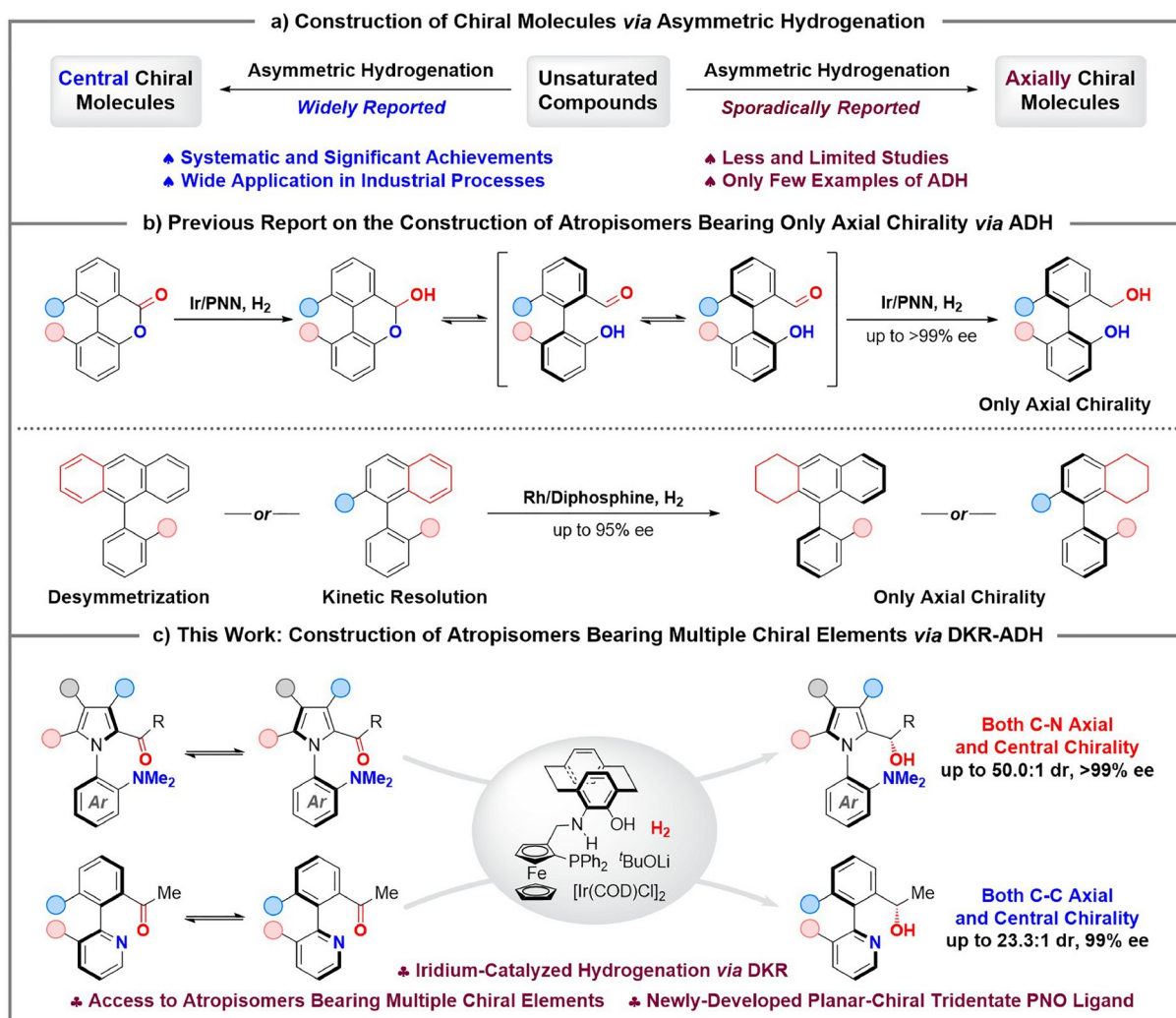
synthesis of enantiomers bearing stereogenic centers has been widely reported. On the contrary, the construction of atropisomers via asymmetric hydrogenation has been relatively less developed [13–24]. These reports mainly focused on the ATH of biaryl aldehydes and biaryl imines. In the presence of chiral phosphoric acids/Hantzsch esters or ruthenium catalysts/azeotrope of formic acid and triethylamine, axially chiral alcohols and axially chiral amines were afforded [13–22]. However, atroposelective ADH using hydrogen gas as the reducing reagent has sporadically been reported (Scheme 1a). In 2018, Zhang's group [23] disclosed an iridium-catalyzed asymmetric direct hydrogenation of Bringmann's lactones, providing atropisomeric biaryl alco-

*Corresponding authors (email: bowu@dicp.ac.cn; ygzhou@dicp.ac.cn)

hols bearing only axial chirality with excellent yields and enantioselectivities (Scheme 1b). They presumed that the lactone was first reduced to hemiacetal, then it quickly isomerized to a configurationally unstable aldehyde, thus the enantiomers are in rapid equilibrium with each other and further ADH produced the final chiral product. In 2022, Zhou's group [24] reported the first rhodium-catalyzed asymmetric hydrogenation of all-carbon aromatic rings, affording a series of axially chiral cyclic compounds with high enantioselectivity through desymmetrization or kinetic resolution (Scheme 1b). Despite these elegant works for the construction of atropisomers bearing only axial chirality via ADH, there still remains a startling lacuna when it comes to the synthesis of atropisomers bearing multiple chiral elements through ADH, which played a crucial role in asymmetric catalysis and medicinal chemistry [25–27].

Dynamic kinetic resolution (DKR), which allows full conversion of racemic substrates into single enantiopure products, is a premier strategy for asymmetric synthesis [28–32]. In the past few decades, DKR has become an efficient

approach for the construction of axially chiral molecules. Noteworthily, DKR enabled by noncovalent interactions opened up a brand-new avenue for the synthesis of axially chiral molecules [33–42], wherein racemization is realized without the need to form and cleave covalent bonds. Instead, the racemization of substrates relies on relatively weak Lewis acid-base interactions. With our long-standing interest in transition metal-catalyzed asymmetric hydrogenation [43–46], we envisioned that the development of asymmetric direct hydrogenation via DKR based on Lewis acid-base interaction would streamline the construction of atropisomers bearing multiple chiral elements. However, without precedent in this field, potential challenges stand in this hypothesis. Evidently, the control of both enantioselectivity and diastereoselectivity represents the most daunting obstacle. Therefore, a catalyst with high catalytic activity and excellent stereoselectivity was deemed indispensable. Herein, we would like to disclose an atroposelective iridium-catalyzed hydrogenation of *N*-arylidole ketones and heterobiaryl ketones via DKR enabled by a newly developed



Scheme 1 (Color online) The construction of atropisomers via asymmetric hydrogenation.

planar-chiral PNO tridentate ligand (Scheme 1c), delivering C–N and C–C atropisomers bearing multiple chiral elements with excellent enantioselectivities and diastereoselectivities simultaneously.

2 Experimental

2.1 General procedure for iridium-catalyzed asymmetric hydrogenation of *N*-arylidole ketones 1

A mixture of $[\text{Ir}(\text{COD})\text{Cl}]_2$ (0.7 mg, 0.5 mol%) and ligand ($S_{\text{FC}}, R_{\text{p}}$)-**L9** (1.4 mg, 1.1 mol%) in 2-methyl-2-butanol (1.0 mL) was stirred in a vial at room temperature for 1 h in a glove box to give the catalyst solution. To another vial was added lithium *tert*-butoxide (0.8 mg, 0.01 mmol), **1** (0.2 mmol), 2-methyl-2-butanol (1.0 mL) and the catalyst solution (1.0 mL). Then the mixture was transferred to an autoclave, which was then charged with hydrogen gas (600 psi), and stirred at 40 °C for 48 h. After careful release of the hydrogen, the autoclave was opened, and the volatiles were removed under reduced pressure. The residue was purified by silica gel column chromatography to give the reductive products **2**. The optical purity of the chiral alcohols was determined by chiral high performance liquid chromatography, and the diastereomeric ratios were determined by proton nuclear magnetic resonance (^1H NMR).

2.2 General procedure for iridium-catalyzed asymmetric hydrogenation of heterobiaryl ketones 3

A mixture of $[\text{Ir}(\text{COD})\text{Cl}]_2$ (0.7 mg, 0.5 mol%) and ligand ($S_{\text{FC}}, R_{\text{p}}$)-**L9** (1.4 mg, 1.1 mol%) in 2-methyl-2-butanol (1.0 mL) was stirred in a vial at room temperature for 1 h in a glove box to give the catalyst solution. To another vial was added lithium *tert*-butoxide (0.8 mg, 0.01 mmol), **3** (0.2 mmol), 2-methyl-2-butanol (1.0 mL) and the catalyst solution (1.0 mL). Then the mixture was transferred to an autoclave, which was then charged with hydrogen gas (600 psi), and stirred at 60 °C for 36 h. After careful release of the hydrogen, the autoclave was opened, and the volatiles were removed under reduced pressure. The residue was purified by silica gel column chromatography to give the chiral reductive products **4**, and the diastereoisomers could be isolated during the column chromatography. The enantiomeric excesses of the chiral alcohols were determined by chiral HPLC, and the diastereomeric ratios were determined by ^1H NMR.

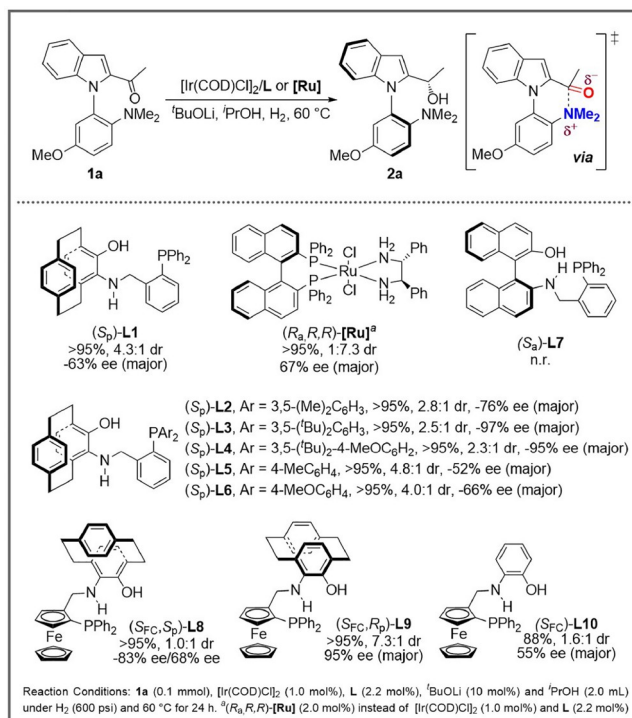
3 Results and discussion

3.1 Reaction optimization

To examine the feasibility of the proposed protocol,

N-arylidole ketone **1a**, which could form a transient Lewis acid-base interaction to accomplish the racemization, was chosen as the model substrate. Initially, this reaction was conducted with the [2,2]-paracyclophane-based planar-chiral tridentate ligands **L1**–**L6** developed in our previous work (Scheme 2) [47]. When **L1** was used as a ligand in the iridium-catalyzed DKR-ADH, **1a** could convert to the axially chiral C–N atropisomer **2a**, which widely exists in natural alkaloids, chiral ligands and chiral organocatalysts [48–50]. However, only moderate ee and dr could be obtained. Further evaluation of **L2**–**L4** showed higher enantioselectivities with increasing steric hindrance of the aryl group in ligands, but erosions of diastereoselectivities were observed disappointingly. With **L5** and **L6** as ligands, similar results were acquired in comparison with **L1**. When applying the BINOL-derived tridentate ligand **L7** to the reaction, no product was observed. On the other hand, the well-known BINAP/1,4-diamine-ruthenium complex developed by Noyori was also tested, although a better dr could be afforded, the enantioselectivity was still not satisfying. As of now, the highest ee was obtained when using **L3** as a ligand (97% ee) in iridium-catalyzed DKR-ADH, and the highest dr was achieved when BINAP/1,4-diamine-ruthenium complex (1:7.3 dr) was applied. Based on these results, we reckoned that a ligand with a suited chiral concave pocket and a better chiral skeleton was fundamental to the improvement of stereoselectivity.

Inspired by the prevalent existence of ferrocene skeleton in chiral ligands and catalysts, we wondered whether ligands combined with the [2,2]-paracyclophane and ferrocene ske-



Scheme 2 (Color online) The evaluation of chiral ligands.

letons would make them adequate candidates in the iridium-catalyzed DKR-ADH of *N*-arylidole ketones. Therefore, (S_{FC},S_p)-**L8** and (S_{FC},R_p)-**L9** which contain two kinds of planar-chiral skeletons were developed and applied in the reaction. We were pleased to find that when (S_{FC},R_p)-**L9** was utilized as a ligand, **2a** could be furnished with 7.3:1 dr and 95% ee, which was the best result among the ligands and catalysts we screened. Additionally, (S_{FC})-**L10** with only ferrocene moiety was synthesized to illustrate the impact of [2,2]-paracyclophane on the control of stereoselectivity. Unsurprisingly, only poor dr and ee could be afforded when ligand (S_{FC})-**L10** was employed. These outcomes elucidated that the newly-developed planar-chiral tridentate PNO ligand (S_{FC},R_p)-**L9** is superior in the control of diastereoselectivity and enantioselectivity at the same time, and these qualities may be attributed to a suited chiral concave pocket and a better chiral skeleton we presumed above.

Subsequently, we evaluated the influence of solvents on the DKR-ADH of **1a** (Table 1). In the presence of lithium *tert*-butoxide under 60 °C, the hydrogenation proceeded

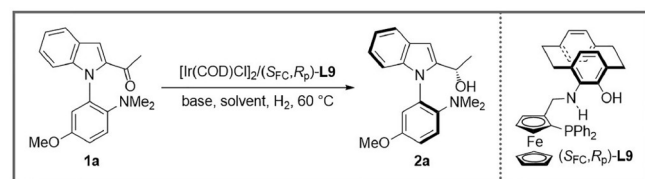
smoothly in THF, and moderate dr and ee were given. In DCE and toluene, **2a** was furnished with low dr and ee. We then turn our attention to various alcohols as solvents to gain a higher level of stereoselectivity. To our delight, excellent reactivities, diastereoselectivities, and enantioselectivities could be obtained in EtOH, ^{*i*}PrOH, ^{*t*}BuOH, and ^{*t*}AmOH (entries 4–7). Through comparison, ^{*t*}AmOH could provide a preferable result (entry 7, 92% yield, 11.5:1 dr, 95% ee), and was chosen as the most suitable solvent. During the screening of base, poor diastereoselectivities were afforded with ^{*t*}BuONa, ^{*t*}BuOK, and NaOH (entries 8–10). The carbonates K₂CO₃ and Cs₂CO₃ were found to be inadequate in this reaction (entries 11 and 12). After further optimization of the catalyst loading and reaction temperature, **1a** could be fully hydrogenated to **2a** with ^{*t*}BuOLi as base, ^{*t*}AmOH as solvent under 40 °C with 1.0 mol% iridium catalyst, giving the **2a** with excellent yield and stereoselectivity (entry 13, 97% yield, 32.3:1 dr, 95% ee).

3.2 Substrate scope

After the establishment of the optimal reaction conditions, we set out to investigate the substrate scope of the DKR-ADH of *N*-arylidole ketones **1**. As shown in Scheme 3, when different electron-donating groups were introduced to *N,N*-dimethylaniline moiety, such as methoxy, ethoxy and phenoxy, the *N*-arylidole ketones were all compatible with the mild reaction conditions, affording the corresponding chiral alcohols with high yields, excellent dr, and ee (92%–99% yields, 12.5:1–33.3:1 dr, 91%–97% ee). For substrate **1b**, the results were not quite satisfactory. This could be interpreted as a harder atropisomerization, which leads to a slight decrease in the stereoselectivity. Substrate **1c** bearing a methyl group instead of an alkoxy group could be hydrogenated smoothly under 60 °C, and affording **2c** with 14.3:1 dr and 94% ee. For the *N*-arylidole ketones bearing a methyl group on different positions of the indole moiety, corresponding chiral alcohols **2h–2j** could be acquired with great yields, dr, and ee (87%–97% yields, 19.0:1–25.0:1 dr, 92%–96% ee). What's more, various alkyls of the ketone moiety were well tolerated, affording **2l** and **2m** with 50.0:1 dr and >99% ee, and **2n** with 33.3:1 dr and 99% ee. For ketone **1p**, which contains trifluoromethyl, **2p** could be furnished with excellent dr, but only 81% ee. Besides, we attempted to expand the DKR-ADH to diaryl ketone, and substrate **1o** was synthesized. Dishearteningly, low reactivity and stereoselectivity were obtained, which might be owing to the minor differentiation of the two aryl groups and a harder atropisomerization. The configuration stability of alcohol **2** was confirmed by heating **2a** in ^{*t*}AmOH (at 80 °C) for 24 h, no erosion of dr and ee was observed in HPLC analysis.

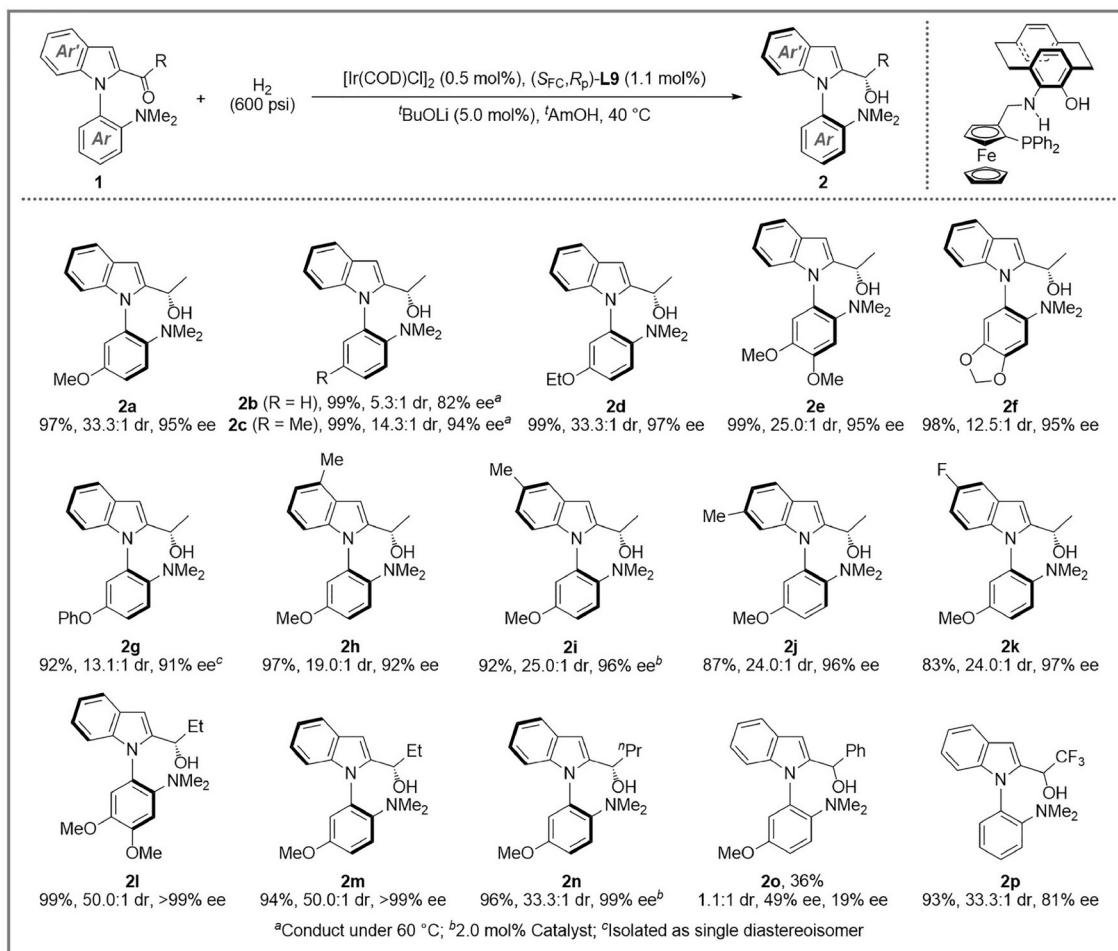
To further demonstrate the validity of this DKR-ADH strategy, the hydrogenation of heterobiaryl ketones was

Table 1 Conditions optimization^{a)}



Entry	Solvent	Base	Yield (%) ^{b)}	dr (%) ^{b)}	ee (%) ^{c)}	
					Major	Minor
1	THF	^{<i>t</i>} BuOLi	>95	4.8:1	88	2
2	DCE	^{<i>t</i>} BuOLi	61	1.9:1	79	–25
3	toluene	^{<i>t</i>} BuOLi	>95	1.6:1	79	–20
4	EtOH	^{<i>t</i>} BuOLi	>95	7.9:1	97	20
5	^{<i>i</i>} PrOH	^{<i>t</i>} BuOLi	>95	7.3:1	95	16
6	^{<i>t</i>} BuOH	^{<i>t</i>} BuOLi	>95	8.8:1	95	53
7	^{<i>t</i>} AmOH	^{<i>t</i>} BuOLi	>95	11.5:1	95	55
8	^{<i>t</i>} AmOH	^{<i>t</i>} BuONa	>95	3.9:1	90	–5
9	^{<i>t</i>} AmOH	^{<i>t</i>} BuOK	>95	2.8:1	93	–27
10	^{<i>t</i>} AmOH	NaOH	>95	2.2:1	90	–6
11	^{<i>t</i>} AmOH	K ₂ CO ₃	n.r.	–	–	–
12	^{<i>t</i>} AmOH	Cs ₂ CO ₃	50	1:1.9	33	–46
13 ^{d)}	^{<i>t</i>} AmOH	^{<i>t</i>} BuOLi	>95	32.3:1	95	34

a) Reaction conditions: **1a** (0.1 mmol), [Ir(COD)Cl]₂ (1.0 mol%), (S_{FC},R_p)-**L9** (2.2 mol%), base (10 mol%) and solvent (2.0 mL) under H₂ (600 psi) and 60 °C for 24 h. b) Yield (total yield of two diastereoisomers) and dr was measured by analysis of ¹H NMR spectra, using 1,3,5-trimethoxybenzene as the internal standard. c) Determined by chiral HPLC. d) Reaction conducted under 0.20 mmol scale, and with [Ir(COD)Cl]₂ (0.5 mol%), **L9** (1.1 mol%) ^{*t*}BuOLi (5 mol%) and ^{*t*}AmOH (2.0 mL) under H₂ (600 psi) and 40 °C for 48 h.



Scheme 3 Substrate scope of *N*-arylindole ketones.

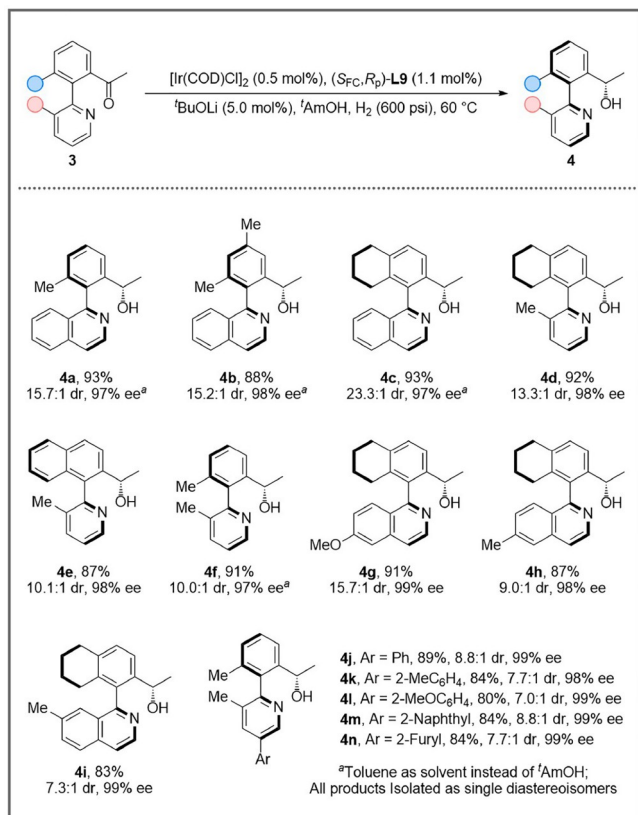
considered as well. On the basis of the established optimal reaction conditions, the substrate scope was evaluated with a fine-tuning of temperature (Scheme 4). The model substrate ketone **3a** could be smoothly converted to the corresponding alcohol **4a** with 93% yield, 15.7:1 dr, and 97% ee for the major diastereoisomer. Similarly, DKR-ADH of heterobiaryl ketone **3b** could afford **4b** with pleasing results. Remarkably, for ketones **3c–3n**, further altering of the ketone moiety or the pyridine moiety led to minor influence on the reactivity and stereoselectivity, furnishing the chiral alcohols **4c–4n** with high yields, diastereoselectivities and excellent enantioselectivities (80%–93% yields, 7.0:1–23.3:1 dr, 93%–99% ee). No significant effect was observed, regardless of electronic properties, steric hindrance, or positions of substituents. The configuration stability of alcohol **4** was demonstrated by Lassaletta and coworkers in their previous work [34].

3.3 Scale-up experiments and synthetic transformations

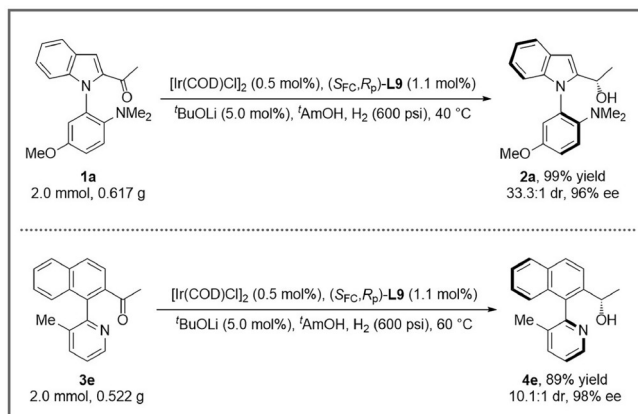
Moreover, scale-up experiments of ketones **1a** and **3e** at 2.0 mmol scale were conducted, respectively. Consistent

results were observed compared to those conducted at 0.2 mmol scale, which demonstrated the potential utility of this DKR-ADH of *N*-arylindole ketones **1** and heterobiaryl ketones **3** (Scheme 5).

To explore the preparative utility of the strategy, we turn our attention to the transformation of the obtained chiral alcohols **2** and **4**, which bear both axial chirality and central chirality (Scheme 6). At first, **2a** could be readily converted to ester **5** with 67% yield and the retentive dr and ee. Furthermore, the absolute configuration of **5** was assigned as (*S_a,S*) by X-ray diffraction analysis (see the Supporting Information online) [51]. Subsequently, the absolute configuration of **2a** was assigned as (*S_a,S*) as well. Unexpectedly, the protection of alcohol **4e** with methanesulfonyl anhydride delivered an olefin, instead of a sulfonate product. We presumed that **4e** might undergo a substitution followed by elimination to afford the olefin product **6**. Luckily, olefin **6** could be furnished with 59% yield and 98% ee. Besides, **4e** underwent the displacement of the primary alcohol using diphenylphosphoryl azide (DPPA) and DBU, followed by Staudinger reduction to furnish the chiral amine **7**. Amine **7** bearing axial chirality and central chirality could be facily



Scheme 4 (Color online) Substrate scope of heterobiaryl ketones.



Scheme 5 Scale-up experiments.

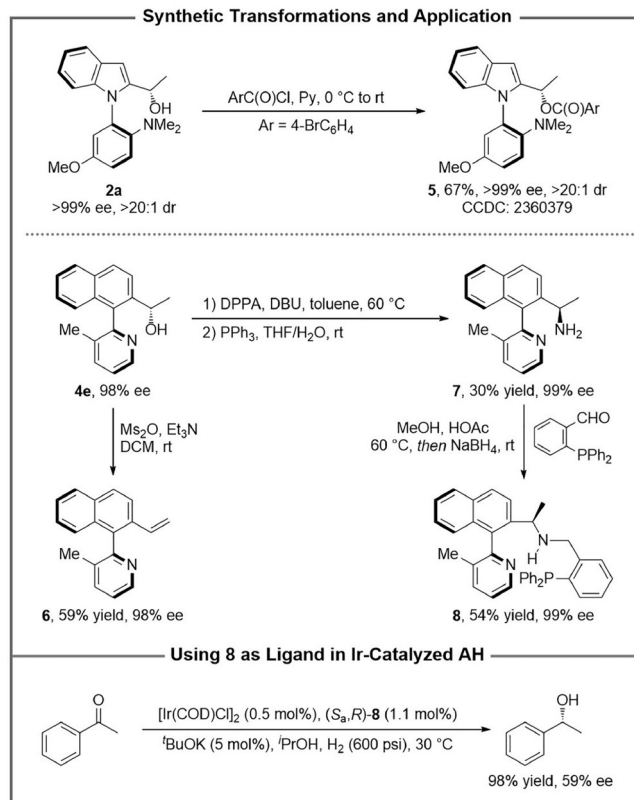
converted to a chiral tridentate PNN ligand **8** with multiple chiral elements through condensation with 2-(diphenylphosphanyl)benzaldehyde. The preliminary application of this newly-developed chiral tridentate PNN ligand was demonstrated in iridium-catalyzed asymmetric hydrogenation of acetophenone, which afforded the 1-phenylethanol with excellent yield and moderate enantioselectivity. Therefore, this kind of heterobiaryl skeleton bearing both axial and central chirality would have promising applications in asymmetric catalysis.

3.4 Proposed reaction model

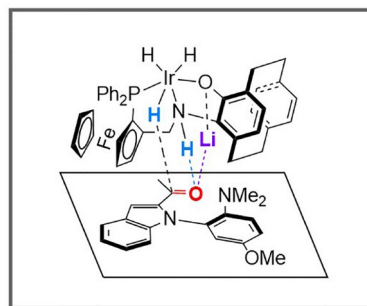
With the confined absolute configuration of **2a** and precedent reports [47,52,53], the reaction model of the DKR-ADH process was proposed in Scheme 7. The deep concave of the chiral ligand and an O–Li···O interaction between the catalyst and substrate were deemed to be responsible for the excellent control of ee and dr at the same time.

4 Conclusions

Taken together, we have developed an atroposelective iridium-catalyzed hydrogenation of *N*-arylindole ketones and heterobiaryl ketones via DKR based on a Lewis acid-base interaction to give the C–N and C–C atropisomers bearing



Scheme 6 Synthetic transformations.



Scheme 7 (Color online) Proposed reaction model.

multiple chiral elements with high yields and stereoselectivities. This strategy presents an unprecedented synthesis of atropisomers bearing multiple chiral elements via ADH [54]. The newly-developed PNO chiral tridentate ligand, which combines the [2,2]-paracyclophane and ferrocene skeleton, is the key feature for this atroposelective hydrogenation, enabling both excellent diastereoselectivities and enantioselectivities. The scale-up experiments and synthetic transformations verified the preparative utility of the DKR-ADH strategy. Further studies are currently underway toward expanding the application of this strategy in the synthesis of prevalent chiral skeletons and bioactive molecules.

Acknowledgements This work was supported by the National Key Research and Development Program of China (2023YFA1507500), the National Natural Science Foundation of China (22171260, 92356302), the Natural Science Foundation of Liaoning Province (2023-MS-009), and the Dalian Institute of Chemical Physics (DICP I202442).

Conflict of interest The authors declare no conflict of interest.

Supporting information The supporting information is available online at <http://chem.scichina.com> and <http://link.springer.com/journal/11426>. The supporting materials are published as submitted, without typesetting or editing. The responsibility for scientific accuracy and content remains entirely with the authors.

- Cerveny L. *Catalytic Hydrogenation*. Amsterdam: Elsevier, 1986
- de Vries JG, Elsevier CJ. *The Handbook of Homogeneous Hydrogenation*. Weinheim: Wiley-VCH, 2007
- Püntener K, Scalone M. Enantioselective hydrogenation: Applications in process R&D of pharmaceuticals. In: Blaser HU, Federsel HJ, Eds. *Asymmetric Catalysis on Industrial Scale: Challenges, Approaches and Solutions*. 2nd ed. Wiley-VCH: Weinheim, 2010
- Noyori R, Hashiguchi S. *Acc Chem Res*, 1997, 30: 97–102
- Tang W, Zhang X. *Chem Rev*, 2003, 103: 3029–3070
- Blaser H, Malan C, Pugin B, Spindler F, Steiner H, Studer M. *Adv Synth Catal*, 2003, 345: 103–151
- Morris RH. *Acc Chem Res*, 2015, 48: 1494–1502
- Wang H, Wen J, Zhang X. *Chem Rev*, 2021, 121: 7530–7567
- Yang F, Xie JH, Zhou QL. *Acc Chem Res*, 2023, 56: 332–349
- Johnson NB, Lennon IC, Moran PH, Ramsden JA. *Acc Chem Res*, 2007, 40: 1291–1299
- Chung JYL, Scott JP, Anderson C, Bishop B, Bremeyer N, Cao Y, Chen Q, Dunn R, Kassim A, Lieberman D, Moment AJ, Sheen F, Zacuto M. *Org Process Res Dev*, 2015, 19: 1760–1768
- Yin C, Jiang YF, Huang F, Xu CQ, Pan Y, Gao S, Chen GQ, Ding X, Bai ST, Lang Q, Li J, Zhang X. *Nat Commun*, 2023, 14: 3718–3725
- Cheng JK, Xiang SH, Li S, Ye L, Tan B. *Chem Rev*, 2021, 121: 4805–4902
- Wang J, Chen MW, Ji Y, Hu SB, Zhou YG. *J Am Chem Soc*, 2016, 138: 10413–10416
- Mori K, Itakura T, Akiyama T. *Angew Chem Int Ed*, 2016, 55: 11642–11646
- Guo D, Zhang J, Zhang B, Wang J. *Org Lett*, 2018, 20: 6284–6288
- Zhang B, Liu L, Guo D, Wang J. *ChemistrySelect*, 2019, 4: 1195–1198
- Carmona JA, Rodríguez-Franco C, López-Serrano J, Ros A, Iglesias-Sigüenza J, Fernández R, Lassaletta JM, Hornillos V. *ACS Catal*, 2021, 11: 4117–4124
- Shao YD, Feng JS, Han DD, Pan KH, Zhang L, Wang YF, Ma ZH, Wang PR, Yin M, Cheng DJ. *Org Chem Front*, 2022, 9: 764–770
- Dai L, Liu Y, Xu Q, Wang M, Zhu Q, Yu P, Zhong G, Zeng X. *Angew Chem Int Ed*, 2023, 62: e202216534
- Jiang H, Han D, Song R, Shi Q, He X, Kou W, Zhao Q, Shao Y, Cheng D. *Adv Synth Catal*, 2023, 365: 1398–1404
- Shao YD, Han DD, Jiang HX, Zhou XY, Wang WK, Zhang JX, Liu YF, Cheng DJ. *Org Chem Front*, 2024, 11: 3894–3899
- Chen GQ, Lin BJ, Huang JM, Zhao LY, Chen QS, Jia SP, Yin Q, Zhang X. *J Am Chem Soc*, 2018, 140: 8064–8068
- Ding Y, Zhu Z, Chen M, Yu C, Zhou Y. *Angew Chem Int Ed*, 2022, 61: e202205623
- Zhang H, Li T, Liu S, Shi F. *Angew Chem Int Ed*, 2024, 63: e202311053
- Yang S, Huang JB, Wang DH, Wang NY, Chen YY, Ke XY, Chen H, Ni SF, Zhang YC, Shi F. *Precision Chem*, 2024, 2: 208–220
- Wu P, Zhang W, Yang J, Yu X, Ni S, Tan W, Shi F. *Angew Chem Int Ed*, 2024, 63: e202410581
- Huerta FF, Minidis ABE, Bäckvall JE. *Chem Soc Rev*, 2001, 30: 321–331
- Bhat V, Welin ER, Guo X, Stoltz BM. *Chem Rev*, 2017, 117: 4528–4561
- Carmona JA, Rodríguez-Franco C, Fernández R, Hornillos V, Lassaletta JM. *Chem Soc Rev*, 2021, 50: 2968–2983
- Pellissier H. *Eur J Org Chem*, 2022, 2022: e202101561
- Moon J, Kim S, Lee S, Cho H, Kim A, Ham MK, Kim SH, Jung J, Kwon Y. *ChemCatChem*, 2024, 16: e202400690
- Carmona JA, Rodríguez-Franco C, Fernández R, Lassaletta JM, Hornillos V. *ChemCatChem*, 2024, 16: e202400701
- Hornillos V, Carmona JA, Ros A, Iglesias-Sigüenza J, López-Serrano J, Fernández R, Lassaletta JM. *Angew Chem Int Ed*, 2018, 57: 3777–3781
- Rodríguez-Salamanca P, de Gonzalo G, Carmona JA, López-Serrano J, Iglesias-Sigüenza J, Fernández R, Lassaletta JM, Hornillos V. *ACS Catal*, 2023, 13: 659–664
- Carmona JA, Rodríguez-Salamanca P, Fernández R, Lassaletta JM, Hornillos V. *Angew Chem Int Ed*, 2023, 62: e202306981
- Rodríguez-Franco C, Ros A, Merino P, Fernández R, Lassaletta JM, Hornillos V. *ACS Catal*, 2023, 13: 12134–12141
- Rodríguez-Franco C, Roldán-Molina E, Aguirre-Medina A, Fernández R, Hornillos V, Lassaletta JM. *Angew Chem Int Ed*, 2024, 63: e202409524
- Coto-Cid JM, de Gonzalo G, Carmona JA, Iglesias-Sigüenza J, Rodríguez-Salamanca P, Fernández R, Hornillos V, Lassaletta JM. *Adv Synth Catal*, 2024, 366: 909–915
- Staniland S, Adams RW, McDouall JJW, Maffucci I, Contini A, Grainger DM, Turner NJ, Clayden J. *Angew Chem Int Ed*, 2016, 55: 10755–10759
- Yuan X, Wang J. *Sci China Chem*, 2022, 65: 2512–2516
- Xu Q, Jia J, Fan H, Ma Z, Wu Y, Zhang Y, Su P, Gao W, Wang Y, Li D. *Org Lett*, 2024, 26: 2403–2408
- Zhou YG. *Acc Chem Res*, 2007, 40: 1357–1366
- Wang DS, Chen QA, Lu SM, Zhou YG. *Chem Rev*, 2012, 112: 2557–2590
- Chen QA, Ye ZS, Duan Y, Zhou YG. *Chem Soc Rev*, 2013, 42: 497–511
- Chen MW, Wu B, Liu Z, Zhou YG. *Acc Chem Res*, 2023, 56: 2096–2109
- Niu T, Liu LX, Wu B, Zhou YG. *J Org Chem*, 2023, 88: 7863–7871
- Zhang HH, Shi F. *Acc Chem Res*, 2022, 55: 2562–2580
- Rodríguez-Salamanca P, Fernández R, Hornillos V, Lassaletta JM. *Chem Eur J*, 2022, 28: e202104442
- Wang J, Wang Z, He W, Ye L. *Chin J Org Chem*, 2024, 44: 1786–1792
- CCDC 2360379 contains supplementary crystallographic data of 5
- Zhang FH, Zhang FJ, Li ML, Xie JH, Zhou QL. *Nat Catal*, 2020, 3: 621–627
- Wang M, Liu S, Liu H, Wang Y, Lan Y, Liu Q. *Nature*, 2024, 631: 556–562
- Wan YB, Hu XP. *ACS Catal*, 2024, 14: 17633–17641